Reflectance-anisotropy spectroscopy and surface differential reflectance spectra at the Si(100) surface: Combined experimental and theoretical study

Maurizia Palummo,[1] Nadine Witkowski,[2,3] Olivier Pluchery,[2,3] Rodolfo Del Sole,[1] and Yves Borensztein[3,2]
[1]*European Theoretical Spectroscopy Facility (ETSF), CNR-INFM, Institute for Statistical Mechanics and Complexity, NAST, via della Ricerca Scientifica 1, 00133 Roma Italy*
and Dipartimento di Fisica, Università di Roma, "Tor Vergata", via della Ricerca Scientifica 1, 00133 Roma, Italy
[2]*University Pierre et Marie Curie-Paris 6, Paris F-75015, France*
[3]*CNRS, UMR7588, Institut des NanoSciences de Paris, 140 rue de Lourmel, Paris F-75015, France*
(Received 18 July 2008; revised manuscript received 29 October 2008; published 30 January 2009)

We present reflectance-anisotropy spectroscopy (RAS) and surface differential reflectivity (SDR) experiments carried out on well-characterized single-domain nominal silicon (100) surface at room temperature. The results are compared with *first-principles* calculations which include many-body effects, namely, self-energy and excitonic effects. These strongly modify the line shape of the optical spectra. For a set of the five measurements, the RAS of clean, monohydride, and dyhidride surfaces, and the corresponding SDRs, good agreement between theory and experiment is obtained only when, in the calculation, the electron-hole interaction is accounted for.

DOI: 10.1103/PhysRevB.79.035327 PACS number(s): 78.68.+m, 71.15.Mb, 71.35.−y

I. INTRODUCTION

In recent years, reflectance-anisotropy spectroscopy (RAS) and surface differential reflectance spectroscopy (SDRS) have been more and more involved in experimental *in situ* surface studies because they are nondamaging, they allow the study of clean and covered surfaces even under nonultrahigh vacuum conditions, and they are sufficiently fast in following real-time surface modifications.[1–3] They have been widely used for investigating semiconductor surfaces, either in clean or during gas adsorptions.[4–9] Nevertheless, since the interpretation of these experiments is generally not straightforward, their full potentiality can be exploited only by a strong interaction of experimental and theoretical works.[1,10] This requires the use of good-quality and well-controlled samples for the experiments, together with the more advanced theoretical approaches in the computational simulations. So far, this combined approach in theory and experiments has been employed in a limited number of cases.[4,11–17] In the present work, we consider the case of Si(100), clean and covered with hydrogen. Set apart as a paradigmatic surface because of its relatively simple reconstruction, Si(100) is a substrate of major importance for development of microelectronic devices, and the control of adsorption of molecules on this surface by means of versatile and easy-to-use optical techniques is promising for applications. Contrary to most of RAS measurements which are performed on vicinal Si(100) surfaces and permitted us to get single-domain samples,[6,18] we have been using here very well oriented nominal Si(100) substrates in order to avoid the presence of steps, which are known to give a non-negligible contribution to the optical response of the surface.[19–21]

Ab initio calculations of surface optical properties are usually carried out at the independent-quasiparticle (I-QP) level. Only in few cases has the electron-hole interaction been included: for instance, strong excitonic effects have been calculated for silicon[13] and germanium (111)2×1 (Ref. 14) surfaces, and giant effects have been obtained for diamond C(100) 2×1,[16] in all cases well explaining the experiments. Instead, no excitonic calculation has been published so far for the prototypical clean silicon (100).

In this work, the RAS and SDRS are measured on the following surfaces: clean Si(100)$c(4\times2)$ surface and monohydride Si(100)2×1:H and dyhidride Si(100)1×1:H surfaces, which were obtained by adsorption of atomic hydrogen at high temperature (585 K) and room temperature (RT), respectively. The results are compared with *ab initio* calculations including all types of many-body effects, namely, self-energy and electron-hole interaction effects, calculated by solving the Bethe-Salpeter equation (BSE).[22,23] This allowed us to obtain a good description of the RAS and surface differential reflectivity (SDR) experiments and permitted us to get a good understanding of the microscopic mode of adsorption of atomic hydrogen as a function of the substrate temperature. In particular, the experimentally observed optical fingerprints previously assigned on a phenomenological basis to the H adsorption, either on the dangling bonds of the Si atoms or in the Si-Si dimers,[24] are now clearly supported by the theoretical results.

II. EXPERIMENTAL

Most optical experiments, dealing with the (100) silicon surface, have been performed up to now, with 4°-misoriented vicinal surfaces. This procedure yields single-domain surfaces formed by narrow terraces separated by double steps, where all Si dimers have the same orientation, which allows one to measure the reflectance anisotropy (RA) induced by the preferential orientation of the dimers. However, the presence of a large number of steps induces an additional anisotropy, as it has been shown experimentally[19] and supported by density functional theory within the local density approximation (DFT-LDA)-based calculations.[20] Moreover, the expected intense surface optical transition located at 1.5 eV, from π bonding states to π^* antibonding states related to the Si-Si dimers, is almost smoothed out because of the narrow

size of the terraces. For these reasons, in the present work we have used very well oriented (better than 0.05°) single crystals of Si(100), which were heated at 1320 K by direct current along the [011] direction through the sample for several hours. The basic pressure was 5×10^{-11} mbar and the maximum pressure did not exceed 5×10^{-10} mbar during the preparation. This procedure has been shown to favor the electromigration of atoms at the surface and to yield the formation of numerous broad terraces, hundreds of nanometers wide in average,[21,25,26] all having the same orientation. Importantly, with this technique, the number of double steps is relatively small and does not influence the optical response of the surface.

Two homemade optical spectrometers have been used for measuring the RAS and the SDRS. The RAS is based on a photoelastic modulator, using the same setup as the one developed by Aspnes *et al.*[27] Working at near-normal incidence, it delivers the reflectance anisotropy defined by

$$\frac{\Delta r}{r} = 2\,\mathrm{Re}\frac{r_{0\bar{1}1} - r_{011}}{r_{0\bar{1}1} + r_{011}}, \tag{1}$$

where the orientations $[0\bar{1}1]$ and [011] are parallel and perpendicular to the dimers, respectively. The reflectances $r_{0\bar{1}1}$ and r_{011} are the complex reflection amplitudes for light polarizations along the two directions. The SDR is performed by the use of a spectrometer based on an optical multichannel analyzer consisting of a Si photodiode array, as described in detail previously.[28] It delivers the relative change in reflectivity of the substrate upon adsorption of H atoms as follows:

$$\frac{\Delta R}{R} = \frac{R_{\mathrm{Si}} - R_{\mathrm{Si:H}}}{R_{\mathrm{Si}}}, \tag{2}$$

where R_{Si} and $R_{\mathrm{Si:H}}$ are the reflectance intensities (i.e., the square of the reflectance in amplitude: $R=|r|^2$) of the clean Si surface and of the H-Si surface, respectively. The measurements presented here were performed at oblique incidence of 45°, in *s* polarization and were normalized to the case of normal incidence for comparison with theory by multiplying them by the factor $\frac{1}{\cos(45)}=\sqrt{2}$. Apart from this factor of cos(45), the measurements are equivalent to the ones which would have been performed at normal incidence.[10] As it will be discussed in more detail below, the actual samples under investigation are composed by majority domains and minority domains, rotated at 90° from the ones to the others, covering about 60% and 40% of the surface, respectively. Figure 1 gives a scheme of the experimental setup, with the Si(100) sample showing majority domains and minority domains. We define direction *X* as the direction of the dimer rows of the majority domains, and direction *Y* as the direction of the dimer rows of the minority domains. As a consequence, the actually measured RA spectra are given by

$$\frac{\Delta r}{r} = 2\,\mathrm{Re}\frac{r_Y - r_X}{r_Y + r_X}, \tag{3}$$

while the SDR spectra were measured with the applied electric field, either along the *X* direction or along direction *Y*. This could be achieved after rotation of the sample by 90° around the normal to the surface. For each SDRS experiment, the sample was cleaned by direct heating and cooled down to the working temperature (room temperature or 585 K) prior to exposure to atomic hydrogen and recording of the SDR spectra. The RAS measurements were performed at room temperature before and after each H adsorption and SDRS measurement.

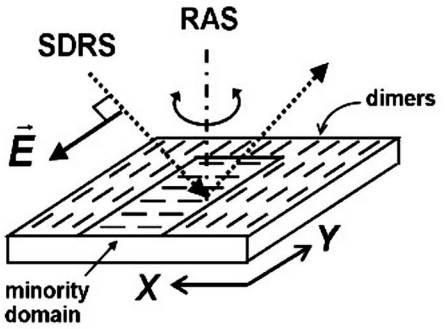

FIG. 1. Experimental setup. Majority and minority domains constituted with dimer rows rotated by 90° are sketched.

III. THEORETICAL APPROACH

Our theoretical *ab initio* approach follows successive steps. First, the geometrical structure of the relaxed ground-state configuration of each surface is obtained, through DFT-LDA calculations,[29] by solving self-consistently the one-particle Kohn-Sham equations.[30] Then the DFT-LDA eigenvalues are corrected by solving the quasiparticle equation within the *GW* approximation.[31] This equation is formally similar to the Kohn-Sham equation, but in place of the local energy-independent exchange-correlation DFT potential, the self-energy operator (which is non-Hermitian, nonlocal, and energy dependent) appears. The calculated quasiparticle energies (i.e., the excitation energies) are the output of this part of the calculation, and with the full dielectric matrix calculated within the random phase approximation (RPA) at the DFT level, they are used as an input of the final calculation, which is the solution of the two-particle BSE that describes the electron-hole pair dynamics.[23,32]

The Si(100) surface is modeled using a repeated slab containing 16 atomic layers and a vacuum region of more than 1 nm. Norm-conserving pseudopotentials[33] for Si and H atoms are employed in both cases. Four $\vec{k}$ points in the irreducible part of the surface Brillouin zone (BZ) are used for the self-consistent calculation of the ground-state charge density. Two hundred uniformly distributed *k* points are used for the 2×1 clean and hydrogenated surfaces while 64 *k* points in the BZ for the $c(4\times2)$ reconstruction for the calculations of the optical properties. We are aware that these samplings are not sufficient to give a complete convergence above 3.5 eV. In particular, it is well known that, for the clean surface, the double negative-positive peak in the E_2 region characteristic of the experimental RAS is reproducible theoretically only with a very dense sampling.[20]

Regarding the *GW* part, the major bottleneck is the computation of the screened interaction *W*. Thanks to previous

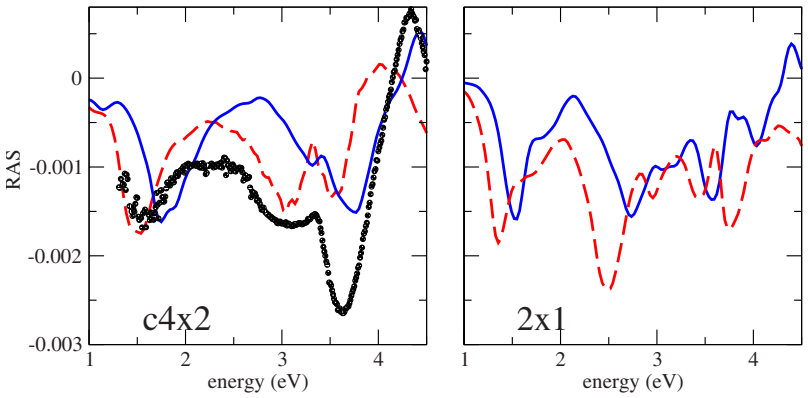

FIG. 2. (Color online) Theoretical RAS calculated for $c(4\times2)$ (left panel) and 2×1 (right panel) Si(100) reconstructions. Solid blue curves are the RAS obtained at the I-QP, while the dashed red curves are those obtained including also the electron-hole interaction. The experimental data are reported only in the left panel as black solid circles. The intensity of the theoretical curves is scaled by a factor of 5.

GW calculations at the Si(100) surface[34] we hypothesized a small dispersion of the self-energy corrections, and we approximated them with a rigid scissor operator of 0.6 eV, as it has been done in other papers.[17,35] In order to eliminate the need to diagonalize the very large nonsparse excitonic matrix (on the order of $100\,000\times100\,000$), we implemented, in a parallel version, the Haydock iterative algorithm proposed by Benedict and Shirley[36] a few years ago in order to solve the Bethe-Salpeter equation. The construction of the excitonic Hamiltonian and the matrix-vector products, needed to apply the Haydock approach, are distributed among different processors.

Excited state calculations based on the mentioned methodology have been successfully carried out since the 1990s in many systems of different dimensionality and generally show important improvements in the description of the optical properties of materials.[22,23] The remaining discrepancies are normally due to computational limits which prevent, like in the present RAS calculations, to achieve a very good convergence in a wide energy range.

IV. RESULTS AND DISCUSSION

A. Reflectance-anisotropy spectra

We now move to the discussion of the experimental curves and their comparison with the theoretical ones. The experimental RAS measured on a clean Si(100) surface at room temperature is reported as black dots on the left panel of Fig. 2. This spectrum is similar in shape and in amplitude to previous experiments performed on nominal samples, prepared either by the same procedure[21,25,26] or by applying a strain at the surface.[19] We have checked using low-energy electron diffraction (LEED) that the surface is not purely 2×1 single domain and that non-negligible 1×2 minority domains are present. This is in contrast with what has been written in Refs. 19 and 25, where it was considered that about 90% of the surface is 2×1 oriented and only 10% with the 1×2 orientation. RAS gives an easy quantitative way of determining with good precision the amount of minority domains on the surface,[21] provided that the RAS of a purely single domain is known. A perfect balance of two domains would lead to a zero RA signal, and balances between majority/minority domains equal to, e.g., 70/30 or 60/40, would give a RA signal identical to the one of a purely single-domain surface but multiplied by a factor equal to 0.4 or 0.2, respectively. The present RAS measurement has the same intensity as in Refs. 19 and 25, which indicates that about the same ratio in average on the whole surface has been obtained in these different experiments. Comparison with the calculation shown later indicates that the ratio of majority/minority domains should be actually on the order of 60/40. Indeed the intensity of the theoretical RAS, presented in the following, is scaled by a factor of 5 to take into account the domains' imbalance. As seen in Fig. 2, the experimental spectrum is dominated by several features: a negative minimum at 1.5 eV, a negative/positive feature at 3.7–4.3 eV, and a negative shoulder around 3 eV.

It is known that the actual room-temperature equilibrium structure of the Si(100) surface has a $c(4\times2)$ order [or a $p(2\times2)$ order], formed by rows of dimers, alternatively buckled along the dimer rows and along the direction perpendicular to the dimer rows (or only along the dimer rows).[37] Because of a temperature-induced "flip-flop" of the dimers at room temperature, scanning tunnel microscope (STM) experiments show an apparent 2×1 order. This is the same with LEED patterns, resulting from space averages of the dimer positions. Molecular-dynamics simulations have shown that a real 2×1 reconstruction starts to occur only at 900 K.[38] Consequently, in order to see if optical measurements are able to distinguish between these reconstructions, we have calculated beyond the one-particle DFT-LDA approach, the RA spectra both for a Si(100)2×1 reconstruction (with dimers buckled in the same direction) and the Si(100)$c(4\times2)$ one.

The *ab initio* RA spectra of the clean silicon (100) surface, calculated at the independent-particle level, have been shown several times in the literature,[20,39] but the effect of the electron-hole interaction, within the BSE framework, has never been considered up to now. In Fig. 2 we report the RA spectra calculated without (blue solid curves) and with the electron-hole (*e-h*) interaction (red dashed curves) for the 2×1 (right panel) and $c(4\times2)$ (left panel) reconstructions of the clean Si(100) surface, together with the experimental RA spectrum on the left panel. The minimum exhibited by all the spectra from 1.3 to 1.7 eV has been clearly attributed to the $\pi-\pi^*$-like transitions, which involve the π-type bonding of the Si-Si dimers.[20,39] Within a simple local scheme of a polarized bond along the dimer, one would expect to excite this optical transition for light polarized along the dimer (in the $[0\bar{1}1]$ direction), which would give a positive feature in the

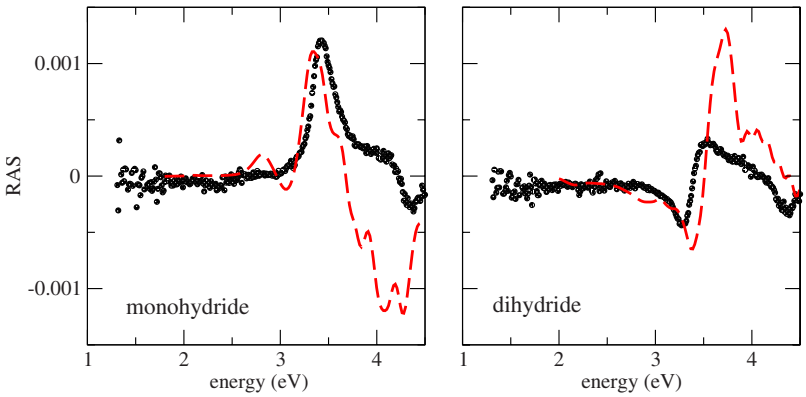

FIG. 3. (Color online) Experimental RA (black dot) and corresponding theoretical BSE spectra (red dashes) for the monohydride and the dyhidride surfaces (left and right panels, respectively). The intensity of the theoretical curves is scaled by a factor of 5, as in Fig. 2.

RA spectrum.[40] However, it has been demonstrated, by *ab initio* calculations[39] that the π electronic states are strongly delocalized along the dimer rows in the [011] direction, which hence yields a negative feature in the RAS. Because of their delocalization, these π states are very sensitive to the quality of the surface (defects, steps, and contamination). In particular, in the case of vicinal (100) surfaces, where the terraces are only 3.9 nm wide in average, this transition is strongly smoothed out and is almost not visible.[21,26]

The I-QP spectrum (blue solid curve) calculated for the 2×1 reconstruction displays a minimum at 2.7 eV, which becomes more intense and is shifted to 2.5 eV when the excitonic effects at the BSE level are included in the calculation (see red dashed curve). This negative peak is not present in the experimental spectrum. Moreover, the strong experimental 3.6–4.3 eV negative-positive feature is also completely absent in the calculated spectra. On the contrary, the $c(4\times2)$ spectra (left panel) display a negative feature around 3.1–3.3 eV, which corresponds to the observed negative shoulder, and the negative-positive feature at higher energy is more visible in this second set of spectra. The better agreement with the experiment of the calculated spectrum for the $c(4\times2)$ with respect to the 2×1 structure is therefore a confirmation that the order of the Si(100) surface at room temperature is $c(4\times2)$.

The next step is the comparison of our results including or not the electron-hole interaction, and we will concentrate on the $c(4\times2)$ spectra on the left panel of Fig. 2. The effect of the *e-h* interaction is minor in the case of $\pi-\pi^*$ transitions located close to 1.5 eV and induces only a redshift of 0.2 eV. The effect is larger for the structures close to 3 eV. The theoretical curve obtained using the BSE approach permits us to better reproduce the negative feature around 3 eV and the sharp positive structure at 3.3 eV. On the opposite, the negative/positive feature at 3.6–4.3 eV is a little less well reproduced when the electron hole is taken into account. However, as indicated above, the limited sampling of k points in the BZ for the $c(4\times2)$ reconstruction prevents a good convergency for high energies and, consequently, the poorer agreement for this feature is not very significant.

It is worthwhile to comment in more detail the shoulder observed experimentally around 3 eV, which is correctly reproduced within the BSE approach. In the case of vicinal Si(100) surfaces, a strong minimum at the same energy was observed and attributed to the presence of numerous double steps at the surface. Consequently, the issue of the origin of this minimum located at the same energy, although much less intense in the case of single-domain surface, was still open. Actually, comparison of RAS on single-domain surfaces measured either in the present work or by some of the present authors previously[21,26] and by two other groups which have measured this quantity[19,25] shows that the intensity of the 3 eV structure with respect to the total intensity of the RA spectrum is the same. This indicates that its origin is intrinsic and not due to a given amount of defects (residual steps) on the surface, possibly caused by some inhomogeneity of the sample, which would not be expected to be the same from one sample to another. Calculations show that it takes its origin essentially from surface-state-to-surface-state transitions with minor contributions of surface-perturbed bulk transitions.[39,41] This feature is most likely related to the 2.8–3 eV peak observed in the SDR spectra measured on the nominal surfaces, as shown in Fig. 4, in agreement with previous SDRS experiments.[42]

At this point, we would like to emphasize the good agreement between RAS of clean Si(100) surface and calculation: the previous comparison shows that in the case of the clean Si(100) surface, as it was already shown for Si(111)2×1, Ge(111)2×1, and C(100)2×1, it is necessary to introduce the electron-hole interaction, within the BSE framework, in order to reproduce correctly the experimental RAS. This better agreement will be confirmed in the following when discussing the SDRS results.

We now discuss the RAS experiments performed after hydrogenation of the surface. The adsorption of atomic hydrogen on the clean Si(100) surface results in two different configurations as a function of the surface temperature during H exposure. When the substrate is maintained around 585 K, the dimers at the surface are preserved and the hydrogen atoms saturate all the dangling bonds of the dimers, leading to a monohydride Si(100)2×1:H surface which has the same 2×1 symmetry as the clean surface, although with symmetric dimers. On the contrary, when the surface is at RT, H atoms break the dimers, leading eventually to a poorly ordered dihydride Si(100)1×1:H surface, where each Si surface atom is now bound to two H atoms.[24,43,44] Figure 3 shows the experimental RA spectra (black dots) obtained for the monohydride (left panel) and the dihydride surfaces (right panel), respectively, measured at room temperature. The corresponding theoretical spectra, obtained including the *e-h* interaction within the BSE framework, are reported for comparison (red dashed curves) in both panels. The first ob-

servation is that the anisotropy signal is strongly reduced with respect to the clean surface and that the $\pi-\pi^*$ transition around 1.5 eV is completely removed, as expected. A peak at 3.4 eV is observed for the monohydride surface, and a derivativelike feature is observed at the same energy for the dihydride one. This energy corresponds to the bulk transitions in silicon at the $E_o'-E_1$ points. These features are therefore due to the effect of the remaining surface anisotropy on the bulk transition in the vicinity of the surface (surface-induced bulk anisotropy[10]). They are remarkably well reproduced by the BSE calculation, with different shapes in both cases. A second weaker feature is observed at 4.3 eV, corresponding to the E_2 bulk transition. The agreement with calculation is not as good as for the 3.4 eV features, especially for the monohydride surface. It has already been indicated that calculations at high energies are less precise because of the limited sampling in the Brillouin zone. It must be noticed that the monohydride surface has been investigated by RAS previously,[45] which was close to the present result, although with some slight differences (an overall negative signal in Ref. 45 which is not present in the RAS shown in Fig. 3 and a stronger 4.3 eV signal than here). These small discrepancies are most likely due to possible different alignments of the optical elements in the RAS apparatus and to different qualities of the hydrogenated surfaces, and they will not be discussed further in the present paper. Finally, we would like to stress that the 3.4 eV feature is observed as a peak for the monohydride surface and that a derivativelike feature is observed for the dihydride surface, prepared on the nominal Si(100) surface. We have shown previously that exactly the opposite behavior was observed on vicinal hydrogenated surfaces.[21,26] It has been shown that the shape of RAS close to the critical points can be either peaklike or derivativelike as a function of the physical processes which are in play, in particular the surface stress.[46–48] It is not one of the purposes of this paper to discuss this question, but a possible explanation could be that the stress at the surface related to the reconstruction and to the presence of hydrogen could be quite different in the case of a nominal surface with a small number of steps and in the case of a vicinal surface with numerous double steps all in the same direction.

B. Surface differential reflectance spectra

We now consider the other set of experiments performed with SDRS. While RAS gives the difference of reflectance between the two main directions of the surface and is measured as well as for the clean and for the hydrogenated surfaces, SDRS delivers the change in reflectance between the clean and the hydrogenated surfaces. Both methods are complementary: RAS gives the subtle difference of reflectance between both directions, which can be a small quantity, if the optical response of the surface is only weakly anisotropic, while SDRS gives the surface optical reflectance of the sample (actually the change due to H adsorption). As it was shown by Del Sole,[10] the different contributions to the surface optical reflectance of a semiconductor surface may originate from transitions between surface states, between surface and bulk states, and from transitions between surface-modified bulk states. The adsorbed H atoms are bound to surface Si atoms and are therefore expected to suppress the Si surface states. Consequently, the SDR spectra obtained after saturation of hydrogen should give mainly the contribution of the surface states of clean Si(100) to the surface reflectance; moreover, as the surface order is modified by the adsorption of H, the surface-modified bulk transitions are also expected to give a contribution.

A recent phenomenological analysis of SDRS upon adsorption of H and of gas molecules on vicinal Si(100) has shown that the surface reflectance is dominated by two broad peaks.[24] The first one, located at about 2.8 eV, is associated to the dangling bonds of the Si dimers and appears when adsorbed atoms or molecules are bonded to the Si atoms of the dimers, while the second one, located at about 3.8 eV, is related to the internal bond between the Si atoms of the dimer and appears only when the dimers are broken because of the adsorption. The present results, obtained on nominal Si(100) surface, show the same behavior. The experimental SDR spectra, after saturation has been reached, are shown on the top panel of Fig. 4. The spectrum involving the monohydride surface (red circles) is characterized by a broad peak at about 2.8 eV and a small shoulder at about 3.6 eV. The SDR of the dihydride surface (black dots) shows two well-pronounced peaks at about 3 and 3.8 eV. The similar behaviors obtained on the vicinal and on the nominal surfaces show that these features are actually related to the Si dimers on the terraces and that the contribution of the steps, in the case of the vicinal surface, is not predominant. The room-temperature spectrum for the dihydride surface displays a clear shoulder around 1.5 eV. In Fig. 4, a SDR spectrum is also drawn, obtained far from saturation, for a smaller amount of adsorbed hydrogen at room temperature (blue stars). It can be seen that only one main peak is observed, centered around 3 eV and that the peak at 3.8 eV characteristic of the dimer breaking is rather weak. This indicates that the surface is an incomplete monohydride surface (about 30%), which is the first stage before reaching the dihydride surface obtained for larger quantities of hydrogen, as we already showed for vicinal surfaces.[24] In this spectrum, the $\pi-\pi^*$ surface-state transition at 1.5 eV is clearly seen, better than in the dihydride surface spectrum, and this will be discussed below in relation to the calculations. This feature is very much sensitive to defects or contamination, and a small amount of adsorbed hydrogen is enough to remove it completely or almost completely (while the 3 eV feature has not yet reached its maximum value), which explains that it is better seen on the slightly exposed surface. A long time ago, Wierenga *et al.*[42] performed similar SDRS experiments on a reduced energy range (1.2–3 eV) by adsorbing molecular oxygen on bidomain nominal surfaces of Si(100). They observed both the 1.5 and the 3 eV peaks, with a larger intensity of the 1.5 eV peak with respect to our case. This can be explained by several reasons: (i) the oxygen adsorption process may be different from the hydrogen one and the results in the incorporation of oxygen atoms in the dimers and in the backbonds, without adsorption on the dangling bonds. Because of the sensitivity of the 1.5 eV transition to contamination and because the 3 eV feature is somehow related to the dangling bonds, the ratio between the 1.5 and the 3 eV

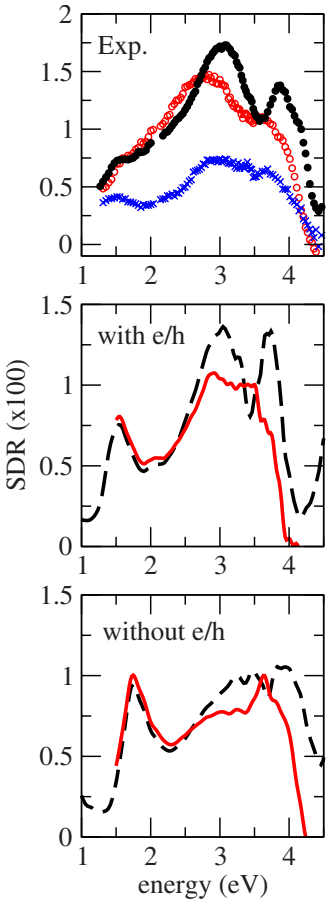

FIG. 4. (Color online) SDR spectra for the mohohydride (red line) and the dihydride (black dashed line) surfaces. The spectra have been averaged on different experiments and on different orientations of the polarization with respect to the dimer rows. Bottom panel: theoretical curves obtained at the independent-quasiparticle random phase approximation (IQ-RPA) level. Central panel: theoretical curves obtained including also the electron-hole interaction at the BSE level. Top panel: experiments performed at room temperature for the dihydride surface (black dot), at 585 K for the monohydride surface (red empty circles), and before saturation at room temperature for the incomplete monohydride surface (blue stars), multiplied by 1.5.

peaks is bigger with adsorption of oxygen than with adsorption of hydrogen. We also performed experiments with oxygen on single-domain nominal surfaces, where at the very beginning of oxygen adsorption the SDR spectrum is dominated by the surface-state transition at 1.5 eV and by the 3.8 eV peak, related to the incorporation of oxygen in the dimers,[49] with only a shoulder at 3 eV. (ii) It is possible that our single-domain nominal surfaces have more defects than the samples studied by Wierenga *et al.*[42] because the procedure we used, in order to perform both RAS and SDRS experiments on the same samples, forced the formation of majority domains with respect to minority ones. The possible bigger amount of defects in our sample should therefore reduce the intensity of the 1.5 eV peak.

The shift of the low energy peak from about 2.95 to 2.8 eV, when comparing the partial monohydride surface obtained by adsorbing atomic hydrogen at room temperature, with the full monohydride surface obtained at 585 K, is most likely due to a temperature effect. We can indeed expect a shift toward lower energies of optical transitions involving surface and bulk states because of electron-phonon interactions.[50] This is the case for purely bulk-to-bulk critical transitions which are redshifted when temperature is increased: the E_0/E_1 critical point is shifted from about 3.4 to 3.25 eV, when going from 300 to 600 K.[51] Purely surface-to-surface transitions are also redshifted with an increase in temperature, as shown on the surface peak measured on the Si(111)2×1 surface.[50,52,53]

SDRS experiments have been performed with light polarized along either the X or the Y directions (Fig. 1). However, the amount of anisotropy of our prepared samples is not big, and the SDR spectra measured in one or the other direction present small differences. Before each SDRS experiment the sample was cleaned by heating, but it is known that this procedure cannot be perfectly reproducible, and the resulting surface displayed some variation from one experiment to another one (number of defects, of steps, of majority/minority domains ratio, etc.). As a consequence, the small differences measured in the SDR spectra for both polarizations X and Y could not be assigned clearly to an effect of surface anisotropy and could originate from variations in the surface quality due to the successive preparations of the sample. In order to avoid such spurious effects, the spectra presented in Fig. 4 have been averaged from several experiments performed in both the X and Y directions. The corresponding calculated spectra, obtained at different levels of approximation, are presented on the central and bottom panels of Fig. 4 for comparison. The bottom panel shows the spectra obtained within the independent-quasiparticle (I-QP) approach, while the central panel reports the theoretical curves obtained including also the electron-hole interaction by using the solution of the Bethe-Salpeter equation. As we can see the overall agreement with the experimental curves is poor at the I-QP level: for the monohydride surface, the main peak is located at 3.6 eV, with a small shoulder at 3 eV and cannot reproduce the main experimental peak at 2.8 eV. The agreement is not better for the dihydride case, showing a broad feature between 3 and 4 eV, without the separation in distinct peaks at 3 and 3.8 eV observed in the experiment.

On the contrary, the agreement is excellent when the excitonic effects are included, both for the monohydride case (one broad peak between 2.7 and 3.5 eV, similar to the experiment) and for the dihydride surface, where the double structures at 3–3.8 eV with the sharp minimum at 3.5 eV are well reproduced. It is worth noticing that the agreement is good, not only regarding the positions of the main peaks but also for the intensity. Contrary to the case of the RAS, where the calculated spectra were more intense than the experimental one, mainly due to the balance between majority 2×1 and minority 1×2 domains, the intensity of the SDRS is very well reproduced by the calculation. This good agreement confirms also that the double-peak spectrum can be considered as the optical "fingerprint" of hydrogen adsorption on Si(100) involving the breaking of the Si dimers, while the single-peak spectrum is the fingerprint of adsorption on dangling bonds, leaving the dimers unbroken.[24]

Finally, the presence of the positive peak in the low-energy part of the spectra, below 2 eV, due to $\pi-\pi^*$ transi-

tions in the clean Si(100)$c(4\times2)$ surface, is visible and very intense in the I-QP spectrum, while it is moved to lower energy in the BSE spectrum and slightly reduced in intensity. Moreover, although the 1.5 eV transition is visible only as a shoulder in the dihydride experimental spectrum for saturation measured at room temperature, it is worth noticing that the shape of the experimental spectrum, for the incomplete monohydride surface obtained at room temperature, where the 1.5 eV feature is proportionally stronger, is close to the BSE calculated curve including electron-hole interaction. On the contrary, the 1.5 eV feature is not or almost visible in the spectrum obtained at high temperature and is not observed anymore at 585 K for smaller amounts of H (not shown here). The 1.5 eV feature, due to transitions between the parallel π and π^* surface bands, is actually very dependent on temperature. We have checked that RAS performed on a nominal Si(100) sample displays this feature at room temperature (Fig. 2), while it is broadened so much that it is almost not visible at 585 K.

V. CONCLUSION

In conclusion this work witnesses the important benefits which can be achieved by a close comparison of surface optical experiments and up-to-date quantum-mechanical calculations. The present *ab initio* calculations, with the inclusion of *e-h* interactions, show how the RAS is sensitive to different surface reconstruction of the clean and covered Si(100) surface, confirming the extreme sensitivity of this optical technique. In particular, regarding the clean surface, we can exclude, thanks to the present study, the presence of a well-ordered 2×1 phase at room temperature. Moreover with the present calculations we confirm the assignment of the two spectral features, at 1.5 and 3 eV, of the $c(4\times2)$ RAS spectrum as due to transitions between surface states. The SDRS measured on the same surface, obtained by subtracting the reflectance of the dyhidride surface from that of the clean surface, shows two peaks at 3 and 3.8 eV which are the optical fingerprints of the saturation of dangling bonds and of dimers breaking, respectively. The SDRS involving the monohydride surface shows only the structure at 3 eV, as a peak, while that at 3.8 eV is only a shoulder. This means that dangling bonds are saturated but that the dimers remain unbroken. These findings are confirmed by the excellent agreement within the many-body theory and the SDR experiments. These results prove that the SDR technique is able to precisely monitor the surface coverage of Si(100). Moreover, it gives access to the absolute value of coverage. Very few experimental techniques can provide this information, and SDRS is probably the easiest to implement. Furthermore, from a theoretical point of view, we have found that excitonic effects are crucial for a correct description of the optical properties of Si(100). They strongly modify RAS and SDR line shapes and are necessary in order to well reproduce the experiments.

ACKNOWLEDGMENTS

This work was funded in part by the EU's Sixth Framework Programme through the Nanoquanta Network of Excellence (Contract No. NMP4-CT-2004-500198). We acknowledge the CINECA CPU time granted by INFM. We also acknowledge partial support from the MIUR program NANOSIM.

[1] P. Chiaradia and R. Del Sole, Surf. Rev. Lett. **6**, 517 (1999).
[2] Y. Borensztein, Surf. Rev. Lett. **7**, 399 (2000).
[3] P. Weightman, D. S. Martin, R. J. Cole, and T. Farrell, Rep. Prog. Phys. **68**, 1251 (2005).
[4] C. Noguez, C. Beitia, W. Preyss, A. I. Shkrebtii, M. Roy, Y. Borensztein, and R. Del Sole, Phys. Rev. Lett. **76**, 4923 (1996).
[5] V. L. Berkovits, N. Witkowski and Y. Borensztein, D. Paget, Phys. Rev. B **63**, 121314(R) (2001).
[6] Y. Borensztein, Phys. Status Solidi A **202**, 1313 (2005)
[7] N. Witkowski, O. Pluchery, and Y. Borensztein, Phys. Rev. B **72**, 075354 (2005).
[8] O. Pluchery, R. Coustel, N. Witkoswki, and Y. Borensztein, J. Phys. Chem. **110**, 22635 (2006).
[9] A. Sassella, A. Borghesi, M. Campione, S. Terrazzi, C. Goletti, G. Bussetti, and P. Chiaradia, Appl. Phys. Lett. **89**, 261905 (2006).
[10] R. Del Sole, in *Photonic Probes of Surfaces*, edited by P. Halevi (Elsevier, Amsterdam, 1995), p. 131.
[11] C. Beitia, W. Preyss, R. Del Sole, and Y. Borensztein, Phys. Rev. B **56**, R4371 (1997).
[12] A. I. Shkrebtii, N. Esser, W. Richter, W. G. Schmidt, F. Bechstedt, B. O. Fimland, A. Kley, and R. Del Sole, Phys. Rev. Lett. **81**, 721 (1998).
[13] M. Rohlfing and S. G. Louie, Phys. Rev. Lett. **83**, 856 (1999).
[14] M. Rohlfing, M. Palummo, G. Onida, and R. Del Sole, Phys. Rev. Lett. **85**, 5440 (2000).
[15] P. H. Hahn, W. G. Schmidt, and F. Bechstedt, Phys. Rev. Lett. **88**, 016402 (2001).
[16] M. Palummo, O. Pulci, R. Del Sole, A. Marini, M. Schwitters, S. R. Haines, K. H. Williams, D. S. Martin, P. Weightman, and J. E. Butler, Phys. Rev. Lett. **94**, 087404 (2005).
[17] P. L. Silvestrelli, O. Pulci, M. Palummo, R. Del Sole, and F. Ancilotto, Phys. Rev. B **68**, 235306 (2003); M. Marsili, N. Witkowski, O. Pulci, O. Pluchery, P. L. Silvestrelli, R. D. Sole, and Y. Borensztein, *ibid.* **77**, 125337 (2008).
[18] L. Kipp, D. K. Biegelsen, J. E. Northrup, L. E. Swartz, and R. D. Bringans, Phys. Rev. Lett. **76**, 2810 (1996).
[19] S. G. Jaloviar, J. L. Lin, F. Liu, V. Zielasek, L. McCaughan, and M. G. Lagally, Phys. Rev. Lett. **82**, 791 (1999).
[20] W. G. Schmidt, F. Bechstedt, and J. Bernholc, Phys. Rev. B **63**, 045322 (2001).
[21] N. Witkowski, R. Coustel, O. Pluchery, and Y. Borensztein, Surf. Sci. **600**, 5142 (2006).
[22] M. Rohlfing and S. G. Louie, Phys. Rev. B **62**, 4927 (2000).
[23] G. Onida, L. Reining, and A. Rubio, Rev. Mod. Phys. **74**, 601 (2002).

[24] Y. Borensztein, O. Pluchery, and N. Witkowski, Phys. Rev. Lett. **95**, 117402 (2005).
[25] R. Shioda and J. van der Weide, Phys. Rev. B **57**, R6823 (1998).
[26] O. Pluchery, N. Witkowski, and Y. Borensztein, Phys. Status Solidi B **242**, 2696 (2005).
[27] D. E. Aspnes, E. Colas, A. A. Studna, R. Bhat, M. A. Koza, and V. G. Keramidas, Phys. Rev. Lett. **61**, 2782 (1988).
[28] Y. Borensztein, T. Lopez-Rios, and G. Vuye, Appl. Surf. Sci. **41-42**, 439 (1989).
[29] First-principles computation of material properties: the ABINIT software project; X. Gonze, J.-M. Beuken, R. Caracas, F. Detraux, M. Fuchs, G.-M. Rignanese, L. Sindic, M. Verstraete, G. Zerah, F. Jollet, M. Torrent, A. Roy, M. Mikami, Ph. Ghosez, J.-Y. Raty, and D. C. Allan, Comput. Mater. Sci. **25**, 478 (2002); code available under http://www.abinit.org
[30] P. Hohenberg and W. Kohn, Phys. Rev. **136**, B864 (1964); W. Kohn and L. J. Sham, *ibid.* **140**, A1133 (1965).
[31] F. Aryasetiawan and O. Gunnarsson, Rep. Prog. Phys. **61**, 237 (1998); Aulbur W. G. Johsson and J. W. Wilkins, in *Solid State Physics*, edited by H. Ehrenreich and F. Spaepen (Academic, New York, 1999).
[32] A. Marini, the YAMBO software project (http://www.yambo-code.org/).
[33] N. Troullier and J. L. Martins, Phys. Rev. B **43**, 1993 (1991).
[34] J. E. Northrup, Phys. Rev. B **47**, 10032 (1993); C. Kentsch, M. Kutschera, M. Weinelt, T. Fauster, and M. Rohlfing, *ibid.* **65**, 035323 (2001).
[35] N. Witkoski, K. Gaal-Nagy, F. Fuchs, O. Pluchery, A. Incze, F. Bechstedt, Y. Borensztein, G. Onida, and R. Del Sole, Eur. Phys. J. B **66**, 427 (2008).
[36] L. X. Benedict and E. L. Shirley, Phys. Rev. B **59**, 5441 (1999).
[37] L. Perdigao, D. Deresmes, B. Grandidier, M. Dubois, C. Delerue, G. Allan, and D. Stievenard, Phys. Rev. Lett. **92**, 216101 (2004); M. Dubois, L. Perdigao, C. Delerue, G. Allan, B. Grandidier, D. Deresmes, and D. Stievenard, Phys. Rev. B **71**, 165322 (2005).
[38] A. I. Shkrebtii, R. Di Felice, C. M. Bertoni, and R. Del Sole, Phys. Rev. B **51**, 11201 (1995).
[39] M. Palummo, G. Onida, R. DelSole, and B. S. Mendoza, Phys. Rev. B **60**, 2522 (1999).
[40] A. I. Shkrebtii and R. Del Sole, Phys. Rev. Lett. **70**, 2645 (1993).
[41] C. Hogan, R. Del Sole, and G. Onida, Phys. Rev. B **68**, 035405 (2003).
[42] P. E. Wierenga, M. J. Sparnaay, and A. van Silfhout, Surf. Sci. **99**, 59 (1980).
[43] J. J. Boland, Surf. Sci. **261**, 17 (1992).
[44] Y. Borensztein and N. Witkowski, J. Phys.: Condens. Matter **16**, S4301 (2004).
[45] R. Shioda and J. van der Weide, Appl. Surf. Sci. **266**, 130 (1998).
[46] D. E. Aspnes, J. Vac. Sci. Technol. B **3**, 1498 (1985).
[47] K. Hingerl, R. E. Balderas-Navarro, A. Bonanni, P. Tichopadek, and W. G. Schmidt, Appl. Surf. Sci. **175-176**, 769 (2001).
[48] Rodolfo Del Sole and Giovanni Onida, Phys. Rev. B **60**, 5523 (1999).
[49] K. Gaál-Nagy, A. Incze, G. Onida, Y. Borensztein, N. Witkowski, O. Pluchery, F. Fuchs, F. Bechstedt, and R. Del Sole, Phys. Rev. B **79**, 045312 (2009).
[50] M. Cardona, Phys. Status Solidi A 188, **1209** (2001).
[51] P. Lautenschlager, M. Garriga, L. Vina, and M. Cardona, Phys. Rev. B **36**, 4821 (1987).
[52] F. Ciccacci, S. Selci, G. Chiarotti, and P. Chiaradia, Phys. Rev. Lett. **56**, 2411 (1986).
[53] M. A. Olmstead and D. J. Chadi, Phys. Rev. B **33**, 8402 (1986).